Heteroatom Chemistry
Volume 20, Number 7, 2009

Stereoselective Synthesis and Antioxidant Activity of Azabicycloadducts Derived from 9,10-Phenanthrenequinone

Komal Arora,[1] D. Jose,[1] D. Singh,[2] R. S. Gupta,[2] P. Pardasani,[1] and R. T. Pardasani[1]

[1]*Department of Chemistry, University of Rajasthan, Jaipur 302 055, India*

[2]*Department of Zoology, University of Rajasthan, Jaipur 302 055, India*

Received 18 December 2008; revised 18 April 2009

ABSTRACT: *A facile synthesis of sprio{1-aza-bicyclo-[3,3,0]-6-octene-8,1′-phenanthrene}-2′-ones has been accomplished by [3 + 2] cycloaddition of azomethine ylide (*amy*) generated from 9,10-phenanthrenequinone and different secondary cyclic amino acids, namely, thiazolidine-4-carboxylic acid,* L*-pyrrolidine-2-carboxylic acid (*L*-proline), and piperidine-2-carboxylic acid (pipecolinic acid) with electron-deficient dipolarophiles in 67%–79% yield. AM1 calculations have been performed to understand the stereochemical course of the cycloaddition. The products have been characterized by elemental analyses and spectroscopic techniques, namely IR,* ^{1}H *NMR, and* ^{13}C *NMR spectroscopies as well as mass spectrometry. Some of the synthesized cycloadducts showed moderate antioxidant activity.* © 2010 Wiley Periodicals, Inc. Heteroatom Chem 20:379–392, 2009; Published online in Wiley InterScience (www.interscience.wiley.com). DOI 10.1002/hc.20562

Correspondence to: R. T. Pardasani; e-mail: rtpardasani@gmail.com

Contract grant sponsor: Department of Atomic Energy/Board of Research in Nuclear Sciences, Mumbai, India.
Contract grant sponsor: University Grants Commission, New Delhi, India.

INTRODUCTION

The monumental work of Huisgen [1] has established 1,3-dipolar cycloaddition reactions as the most powerful methodology for the construction of five-membered heterocycles [2]. The biological importance of pyrrolidines [3] has also inspired the development of [3 + 2] azomethine ylide cycloadditions. In this context, we have examined [3 + 2] cycloaddition reactions of indole-2,3-dione and benzo[β]thiophene-2,3-dione with various secondary cyclic amino acids [4]. However, the work on 9,10-phenanthrenequinone has remained unexplored. The fact that phenanthrenequinone derivatives have been reported to possess strong antioxidant properties [5] including free radical scavenging activity and can reduce lipid peroxidation prompted us to investigate cycloaddition reactions of azomethine ylides derived from phenanthrenequinone and various pharmacologically active secondary cyclic amino acids, namely thiazolidine-4-carboxylic acid (TCA), L-proline and piperidine-2-carboxylic acid (PCA) [6]. Literature survey revealed that TCA exhibits strong antioxidant properties [7]. It has been reported as an intracellular sulfhydryl antioxidant and free radical scavenger [8]. Dietary supplementation with thiaproline improves immune response (leukocyte function) [9] as well as stimulates the phagocytic process of macrophages [10], and neutralization of the superoxide radical is also observed [11]. Therefore,

any heterocyclic system incorporating these two moieties might be expected to have significant biological activities. The results are reported herein.

RESULTS AND DISCUSSION

The reaction of phenanthrenequinone **1** with (*R*)-thiazolidine-4-carboxylic acid (TCA) **2a**, L-pyrrolidine-2-carboxylic acid (L-proline) **2b**, and PCA **2c** in equimolar ratio in refluxing acetonitrile for 22 h generated, in situ, azomethine ylide (Scheme 1) **3a–c**, which was trapped as cycloadduct in the presence of various dipolarophiles, namely phenyl acetylene, diphenyl acetylene, 1-phenyl-1-propyne, ethyl phenyl propiolate thereby producing azabicycloadducts **4a–7c** in 67%–80% yields.

Repeating the reaction with methyl acrylate afforded **8a–c** in 73%–78% yields, respectively. The product distribution is given in Table 1.

The mechanism for the formation of cycloadducts involves the formation of intermediate azomethine ylide (*amy*) **3a–c** formed during the reaction by the loss of CO_2 via a stereospecific cycloreversion [12], which subsequently undergoes 1,3-dipolar

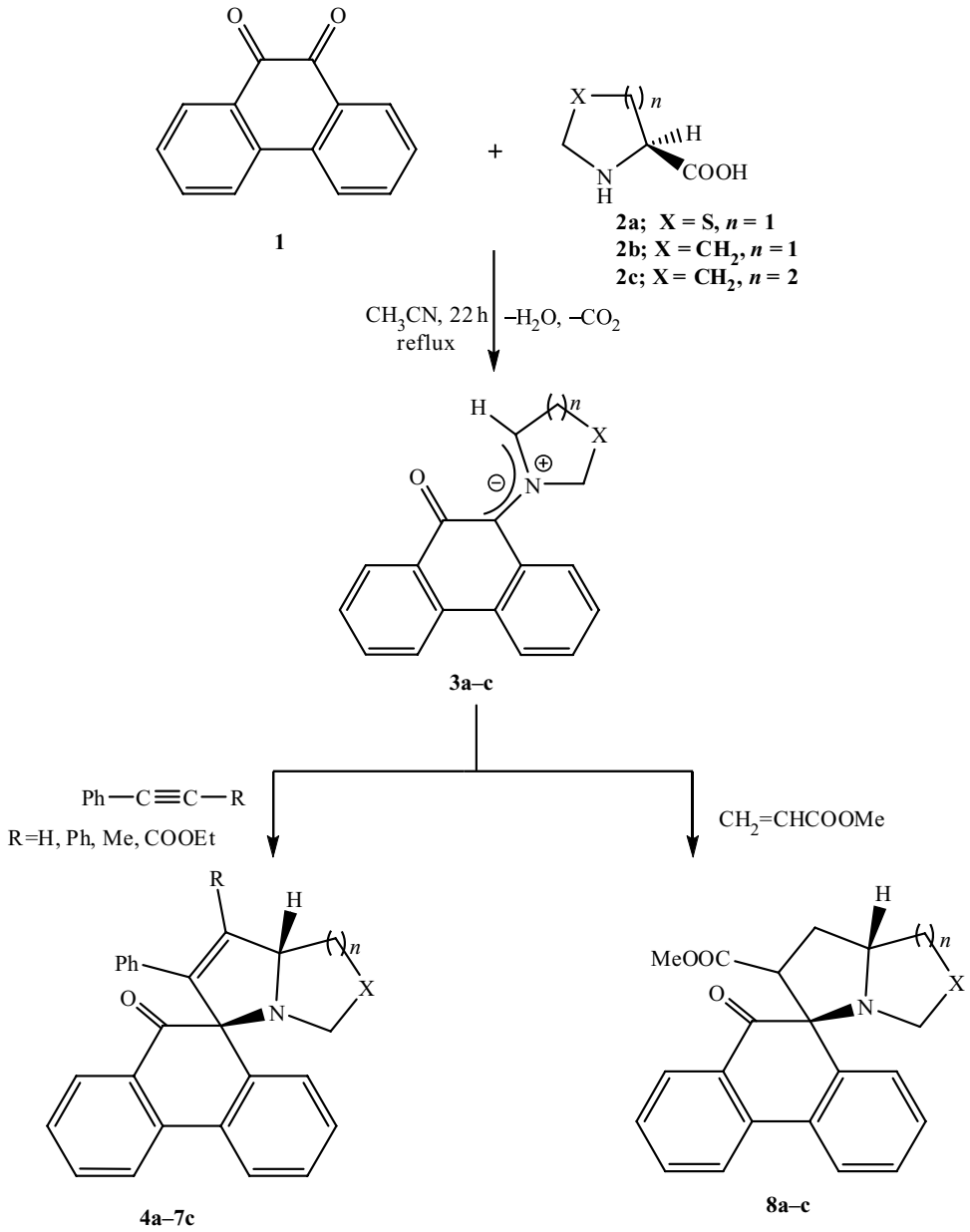

SCHEME 1 Reaction of 9,10-pheanthrenequinone with α-amino acids (**2a–c**) in the presence of different dipolarophiles.

TABLE 1 Product Distribution of Synthesized Azabicycloadducts

Cycloadduct	*Amino Acid*	*Dipolarophile Ph—C≡C—R, R =*	*Cycloadduct*	*Amino Acid*	*Dipolarophile Ph—C≡C—R, R =*
4a	2a	H	**6a**	2a	Me
4b	2b	H	**6b**	2b	Me
4c	2c	H	**6c**	2c	Me
5a	2a	Ph	**7a**	2a	COOEt
5b	2b	Ph	**7b**	2b	COOEt
5c	2c	Ph	**7c**	2c	COOEt

cycloaddition reactions with various dipolarophiles, giving regiospecific spiro compounds. The results are in good harmony with the observation of Grigg et al. [13, 14] for the reaction of carbonyl compounds with amines as well as with the theoretical calculations.

The structure of compounds has been established from their spectral data. The IR spectrum of the typical phenyl acetylene cycloadduct **4a** (where R = H) showed characteristic bands at 1675, 1290, and 650 cm^{-1} for >C=O, C—N, and C—S stretching vibrations, respectively. Its ^1H NMR spectrum showed a quartet at δ 1.86 for 5-H, a doublet at δ 2.25 for 4-H, a broad multiplet at δ 2.90 for 2-H + 6-H; aromatic protons were seen as multiplet in the range δ 7.26–8.21 ppm. Its ^{13}C NMR spectrum displayed a signal at 180.2 for carbonyl carbon, aromatic carbons appeared in the range δ 136.0–128.3 ppm, the olefinic carbons appeared at δ 128.2 and 123.9, and spiro carbon appeared at δ 89.5, C-5 at δ 66.6, C-2 at δ 59.0 and C-4 at 49.0 ppm. Additional evidence was gathered from its mass spectrum. The molecular ion peak and base peaks were present at *m/z* 381 (35%) and *m/z* 279 (100%), respectively. The mass fragmentation pattern has been depicted in Scheme 2. Physical and spectral data have been given in the Experimental section, respectively.

MOLECULAR ORBITAL ANALYSIS

Detailed semiempirical molecular orbital studies were conducted employing MOPAC 6 program on AM1 Hamiltonians to understand the stereochemical course of the cycloaddition reaction. Geometry optimization of azomethine ylide **3a** indicated that it has an almost planar structure (Fig. 1).

Instead of having an envelope shape, the thiaproline ring is planar and lies in the same plane as that of phenanthrenequinone ring. It may exist as two conformers, one in which the >C=O group and C—H of the dipole are syn to each other $\mathbf{3a}_{syn}$ and the other one in which these two groups are *anti* $\mathbf{3a}_{anti}$ (Fig. 2).

Phenyl acetylene may approach either of the azomethine ylide (*amy*) syn or anti with the formation of products having two chiral centers. Therefore, a total of 4 + 4 = 8 stereoisomers could be possible (Fig. 3).

Attack of phenyl acetylene on *anti*-azomethine ylide (anti amy) results in the inward movement of thiazolidine ring toward the phenanthrene nucleus, and the transition state (TS) could not be located even in a single case (Fig. 2). It may be due to the steric hindrance between the quinone nucleus and the thiaproline ring that makes it unstable and hence fails to produce transition state geometry, ruling out the possibility of formation of products **[4a(v)–4a(viii)**]. Thus it leaves the possibility of attack on only the *syn* azomethine ylide (amy) and hence only four isomers **4a(i)–4a(iv)** are left for consideration. Out of these four possibilities, only

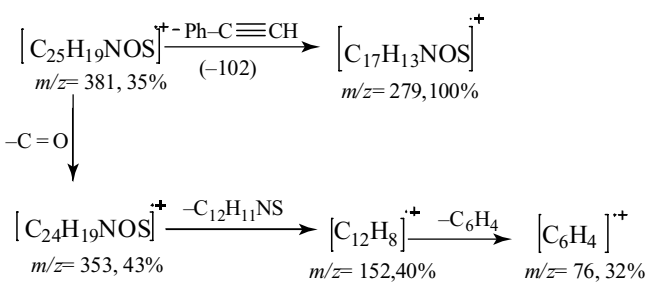

SCHEME 2 Mass fragmentation pattern of phenyl acetylene cycloadduct **4a**.

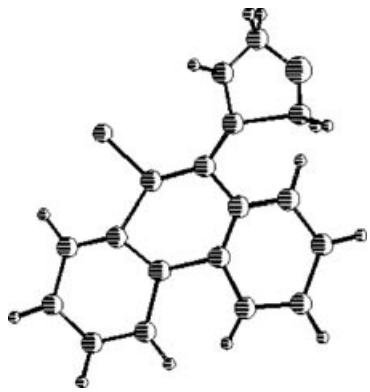

FIGURE 1 AM1-optimized geometry of azomethine ylide **3a**.

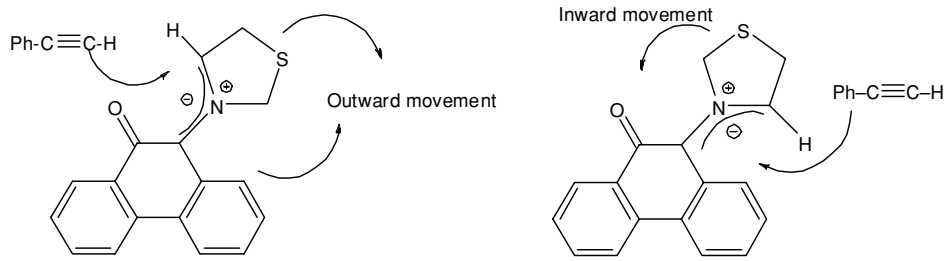

FIGURE 2 Mode of attack of dipolarophile (phenyl acetylene) on azomethine ylide.

two have concerted mechanism **4a(i)** and **4a(ii)** and we could optimize the transition state in the case of **4a(i)** only. This can be explained using the frontier molecular orbitals (FMO) approach along with the endo approach of the phenyl ring. The favored path involves the $HOMO_{dipole}$ and $LUMO_{dipolarophile}$. The transition state of the concerted 1,3-dipolar cycloadditions is usually controlled by FMOs of dipolarophiles and dipole (azomethine ylide).

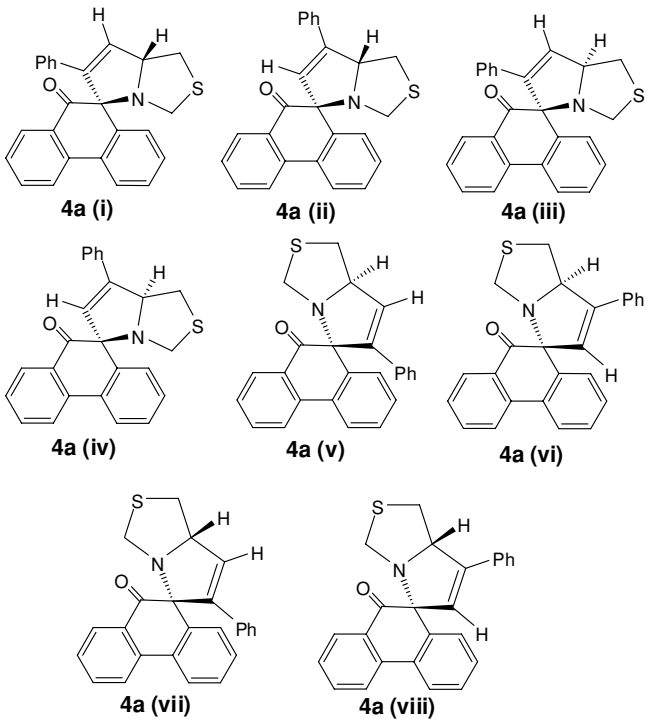

FIGURE 3 Possible stereoisomers of cycloadduct **4a**.

The ΔH_f, HOMO, LUMO energies, and HOMO–LUMO energy gaps of azomethine ylides **3a–c** with dipolarophiles are given in Table 2. From the table, it may be concluded that $HOMO_{dipole}$–$LUMO_{dipolarophile}$ energy gap is lower than the $LUMO_{dipole}$–$HOMO_{dipolarophile}$ gap and therefore the dominant FMO approach is $HOMO_{dipole}$–$LUMO_{dipolarophile}$.

Both the HOMO and the LUMO of the dipole show uneven distribution of the electron density along the C—N—C dipole. In the HOMO case, the orbital coefficient is larger at C_1 (0.229) than at C_2 (−0.162). Similarly in the LUMO of phenyl acetylene, the atomic orbital coefficient on the C-atom bearing the phenyl group is larger (0.202) than that of the atom away from it (−0.142). Thus, there is a better orbital overlap between C_1 of azomethine ylide and the C-atom bearing the phenyl group. (Fig. 4)

This results in the formation of product **4a(i)**, thus ruling out the possibility of **4a(ii)**, in which case we could not optimize the transition state. Besides a secondary interaction between the two phenyl rings, the endo approach also favors the formation of product **4a(i)**. The AM1-optimized geometry of cycloadduct **4a** and energy profile diagram for the

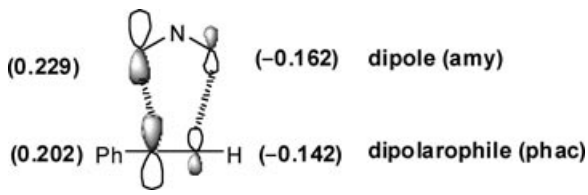

FIGURE 4 Atomic orbital coefficients and overlapping of dipole (**3a**) with dipolarophile (phac).

TABLE 2 ΔH_f, HOMO, LUMO Energies and H-L and L-H Energy Gaps

				Energy Gaps (ev)	
	ΔH_f (Kcal/mol)	HOMO (ev)	LUMO (ev)	H-L	L-H
Dipole azomethine ylide (**3a**)	74.85	−7.71	−0.97	–	–
Dipolarophiles					
phac	74.65	−9.39	−0.07	7.64	8.42
diph	97.81	−8.75	−0.44	7.27	7.78
phpr	64.88	−9.08	−0.03	7.68	8.01
etph	−10.80	−9.71	−0.66	7.05	8.74
meac	−65.98	−11.06	−0.06	7.65	10.09
Dipole azomethine ylide (**3b**)	59.72	−7.44	−0.60	–	–
Dipolarophiles					
phac	74.65	−9.39	−0.07	7.37	8.79
diph	97.81	−8.75	−0.44	7.00	8.15
phpr	64.88	−9.08	−0.03	7.41	8.48
etph	−10.80	−9.71	−0.66	6.78	9.11
meac	−65.98	−11.06	−0.06	7.38	10.46
Dipole azomethine ylide (**3c**)	48.14	−7.38	−0.58	–	–
Dipolarophiles					
phac	74.65	−9.39	−0.07	7.31	8.80
diph	97.81	−8.75	−0.44	6.94	8.16
phpr	64.88	−9.08	−0.03	7.35	8.50
etph	−10.80	−9.71	−0.66	6.64	9.13
meac	−65.98	−11.06	−0.06	7.32	10.48

phac = phenyl acetylene; diph = diphenyl acetylene; phpr = 1-phenyl-1-propyne; etph = ethylphenyl propiolate; meac = methyl acrylate.

cycloadducts **4a, 5a, 4b, 5b, 4c**, and **5c** have been depicted in Figs. 5 and 6, respectively.

ΔH_f-R, ΔH_f-TS, ΔH_f-P, E_a, and stabilization energy of azomethine ylide with different dipolarophiles are presented in Table 3.

Parallel calculations have been performed on other cycloadducts, and the following conclusions may be drawn:

1. Geometry optimization of the azomethine ylide **3a** indicated that it has an almost planar structure. The thiaproline ring, instead of having an envelope shape, is planar and lies in the same plane as that of the phenanthrene moiety.

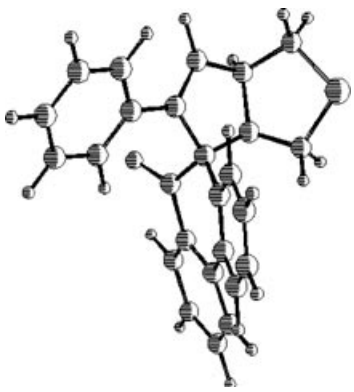

FIGURE 5 AM1-optimized geometry of phenyl acetylene cycloadduct **4a**.

2. The dominant FMO approach is $HOMO_{dipole} - LUMO_{dipolarophile}$ as this energy gap is lower than the $LUMO_{dipole} - HOMO_{dipolarophile}$ gap.
3. The endo approach is favored, and the phenyl group lies toward the phenanthrene ring.

ANTIOXIDANT ACTIVITY

Free radicals are highly reactive species owing to the presence of unpaired valence shell electron and possess damaging activity toward macromolecules such as protein, DNA, and lipids [15].

Antioxidants and radical scavengers have been employed to study the mechanism of CCl_4 toxicity as well as to protect liver cells from CCl_4-induced damage by breaking the chain reaction of lipid peroxidation [16]. Therefore, the present study aimed to establish the antioxidant potential of azabicycloadducts derived from 9,10-phenanthrenequinone, using CCl_4-induced peroxidative damage in rats. Initially, a control experiment was performed with known antioxidant silymarin to facilitate standardization of the data with following test compounds.

The two compounds selected for the present study are compound I: (5*S*, 8*R*)-spiro-{6,7-diphenyl-1-aza-3-thia-bicyclo-[3,3,0]-6-octene-8,1′-phenanthrene}-2′-one (**5a**) and compound (II):

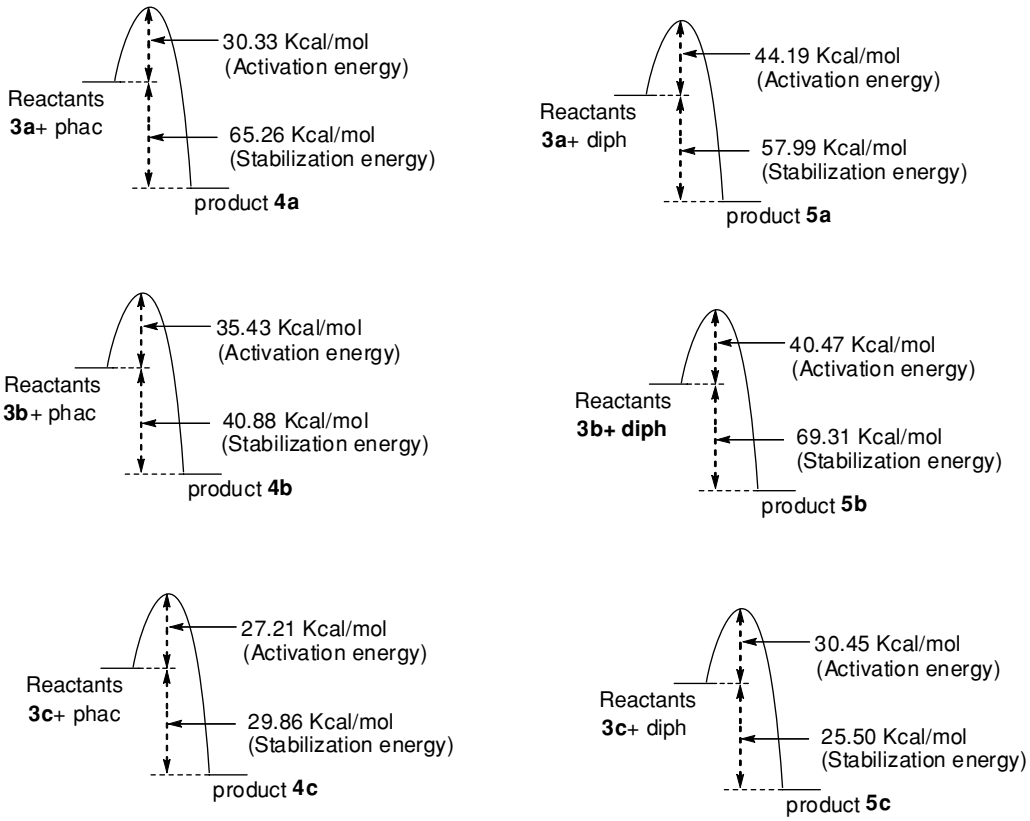

FIGURE 6 Energy profile diagram of cycloadducts **4a, 5a, 4b, 5b, 4c**, and **5c**.

(5*S*, 8*R*)-spiro-{6-ethoxycarbonyl-7-phenyl-1-aza-3-thia -bicyclo-[3,3,0]-6-octene-8,1′-phenanthrene}-2′-one (**7a**).

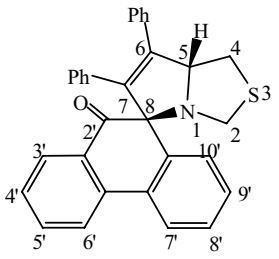

5a

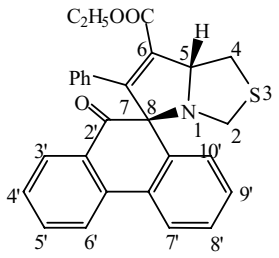

7a

Results

The results of biochemical and histological parameters revealed that the administration of CCl_4 to rats caused significant ($p \leq 0.001$) oxidative damage as evidenced by marker enzymes, antioxidant defense system, and histo-architectural examinations through liver and serum contents (Table 4 and Figs. 7–11).

Rats treated with CCl_4 showed a significant ($p \leq 0.001$) elevation in serum enzymatic activities of SGOT (serum glutamic oxaloacetic transaminase), SGPT (serum glutamic-pyruvic transaminase), ALP (alkaline phosphatase), and total bilirubin when compared with normal vehicle controls (group 1). The oral administration of compound **5a** and **7a** attenuated the CCl_4-induced rise in the SGOT, SGPT, ALP, and total bilirubin levels (groups IV and V) when compared with group II (the CCl_4-treated group) (Table 4). The attenuation of enhanced SGOT, SGPT, ALP, and total bilirubin level by compounds **5a** and **7a** was statistically similar in nature with the standard drug silymarin (known antioxidant), thus suggesting that the test compounds are as active as the standard and hence may prove to be potential antioxidant agents.

TABLE 3 ΔH_f-R, ΔH_f-TS, ΔH_f-P, E_a, and Stabilization Energy of Azomethine Ylide with Different Dipolarophiles

		ΔH_f (kcal/mol)				
Compound	*Reactants*	*R*	*TS*	*P*	E_a *(kcal/mol)*	*Stabilization Energy (kcal/mol)*
4a	**3a** + phac	149.50	179.83	84.24	30.33	65.26
5a	**3a** + diph	172.66	216.85	114.67	44.19	57.99
7a	**3a** + etph	64.05	98.42	25.03	34.67	39.02
4b	**3b** + phac	134.37	169.80	93.49	35.43	40.88
5b	**3b** + diph	157.52	197.99	89.21	40.47	69.31
6b	**3b** + phpr	124.60	158.28	86.14	33.68	38.46
4c	**3c** + phac	122.79	150.00	90.93	27.21	29.86
5c	**3c** + diph	145.95	176.40	120.45	30.45	25.50
6c	**3c** + phpr	113.02	144.50	78.04	31.48	34.98
7c	**3c** + etph	37.34	61.59	7.55	24.25	29.79

phac = phenyl acetylene; diph = diphenyl acetylene; etph = ethylphenyl propiolate phpr = 1-phenyl-1-propyne; E_a = activation energy.

Table 4 depicts that the activities of hepatic antioxidants such as SOD (superoxide dismutase), CAT (catalase), GSH (reduced glutathione), and lipid peroxidation (LPO) were altered significantly ($p \leq 0.001$) upon CCl_4- induction to rats (group II) when compared with group I (vehicle control). In contrast, treatment with compounds **5a** and **7a** (10 mg/kg) showed a significant restoring effect on CCl_4-induced peroxidative damage (groups IV and V). The restoration of hepatic peroxidative damage by compounds **5a** and **7a** at the dose level of 10 mg/kg statistically showed equal protection vis-à-vis as good as silymarin (10 mg/kg) (group III of known antioxidant).

Histology of the liver sections of normal control animals (Fig. 7) showed normal hepatic cells with well-preserved cytoplasm, prominent nucleus, nucleolus, and visible central veins. The liver

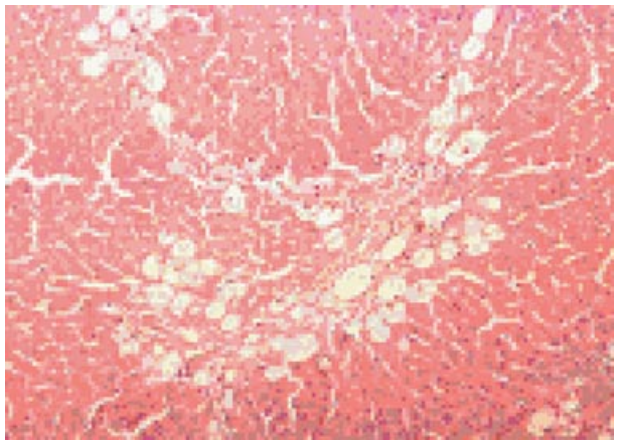

FIGURE 8 Photomicrograph of rat liver section with CCl_4 treatment showing marked steatosis of the hepatocytes with ballooning degeneration and distended portal vein, mild periportal fibrosis, and necrosis at H & E × 100.

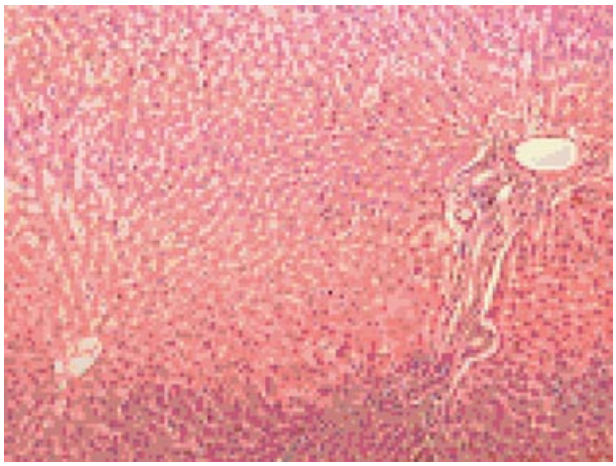

FIGURE 7 Photomicrograph of control rat liver section showing well brought central vein, hepatic cells with preserved cytoplasm, and prominent nucleus at hematoxylin and eosin (H & E) × 100.

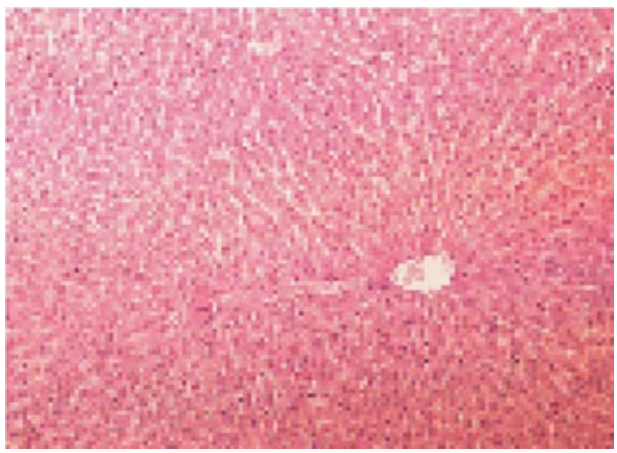

FIGURE 9 Photomicrograph of rat liver section of CCl_4 + silymarin (10 mg/kg body weight), showing histological pattern almost similar to liver of vehicle-treated rats with preserved cytoplasm and prominent nucleus at H & E × 100.

TABLE 4 Antioxidant Activity of Standard Drug Silymarin and Compounds **5a** and **7a** against CCl_4-Induced Oxidative Stress in Rats through Various Biochemical Parameters

	Serum				*Tissue*			
Groups	*SGOT (U/L)*	*SGPT (U/L)*	*ALP (KAU)*	*Total Bilirubin (mg/dL)*	*SOD (μmol/ mg protein)*	*CAT (μmol H_2O_2 consumed/min/ mg protein)*	*GSH (nmol/g tissue)*	*LPO (nmol MDA/mg tissue)*
Group I: Normal	130.13 ± 3.98	118.40 ± 2.42	13.40 ± 1.30	0.67 ± 0.09	9.85 ± 0.49	64.45 ± 3.42	3.82 ± 0.17	2.10 ± 0.14
Group II: CCl_4	$320.12 \pm 5.10^{**}$	$285.15 \pm 4.49^{***}$	$28.17 \pm 2.18^{***}$	$1.95 \pm 0.16^{***}$	$2.98 \pm 0.14^{***}$	$28.10 \pm 1.85^{***}$	$1.21 \pm 0.09^{***}$	$6.33 \pm 0.59^{***}$
Group III: Control experiment (CCl_4 + silymarin)	151.14 ± 2.52^{a}	139.10 ± 2.48^{a}	16.14 ± 1.10^{a}	0.80 ± 0.09^{a}	8.02 ± 0.16^{a}	55.28 ± 2.12^{a}	3.30 ± 0.15^{a}	3.05 ± 0.19^{a}
Group IV: CCl_4 + compound **5a**	192.15 ± 3.10^{a}	173.10 ± 2.45^{a}	18.20 ± 1.85^{b}	0.97 ± 0.11^{a}	6.98 ± 0.20^{a}	49.15 ± 5.10^{a}	3.09 ± 0.12^{a}	3.62 ± 0.33^{b}
Group V: CCl_4 + compound **7a**	169.17 ± 2.92^{a}	149.15 ± 2.32^{a}	17.13 ± 1.17^{a}	0.84 ± 0.10^{a}	7.82 ± 0.19^{a}	53.14 ± 2.32^{a}	3.24 ± 0.18^{a}	3.23 ± 0.24^{a}

Levels of significance: Data are mean $\pm$ SEM ($n = 6$).
$^{***}P \leq 0.001$ group II compared with control (group I).
$^{a}P \leq 0.001$.
$^{b}P \leq 0.01$ groups III, IV, and V compared with group II.

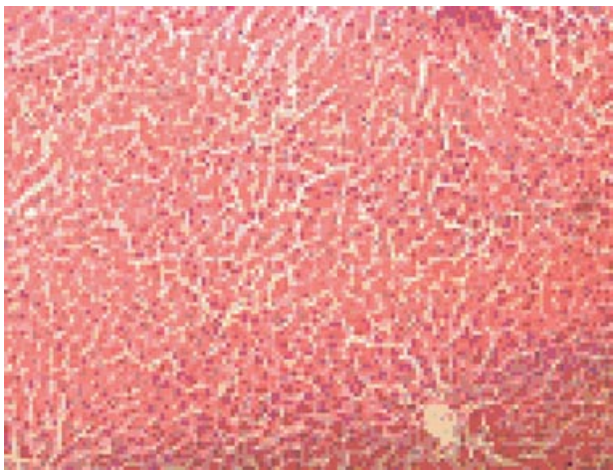

FIGURE 10 Photomicrograph of rat liver section of CCl_4 + compound **5a** (10 mg/kg body weight), showing considerable reduction in necrosis and fatty changes with pyknotic nuclei and cytoplasmic clearing at H & E × 100.

sections of CCl_4-intoxicated rats showed massive fatty changes, necrosis, ballooning, degeneration, and broad infiltration of the lymphocytes and loss of cellular boundaries (Fig. 8). The histological architecture of the liver sections of the rats treated with silymarin and test compounds **5a** and **7a** showed more or less normal lobular pattern with a mild degree of fatty changes, necrosis, and lymphocyte infiltration almost comparable to the normal control (Figs. 9–11).

Discussion

Antioxidants may offer resistance against the peroxidative damage by scavenging the free radicals,

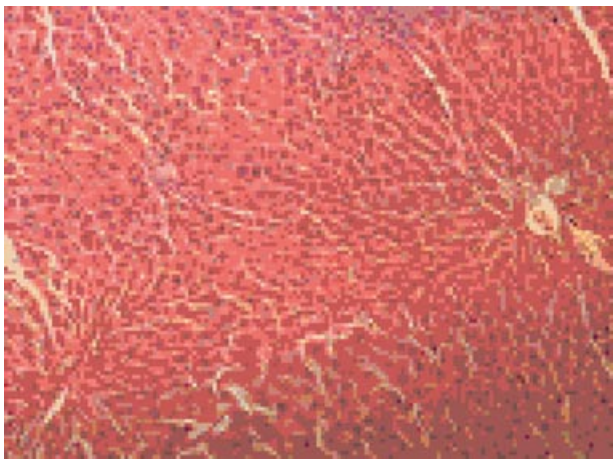

FIGURE 11 Photomicrograph of rat liver section of CCl_4 + compound **7a** (10 mg/kg body weight), showing moderately regeneration in hepatocellular architecture at H & E × 100.

inhibiting the lipid peroxidation and by many other mechanisms and thus preventing diseases [17]. CCl_4-induced hepatotoxicity begins with the changes in endoplasmic reticulum, which result in the loss of metabolic enzymes located in the intracellular structures [18]. The toxic metabolite $CCl_3^{\bullet}$ radical is produced, which further reacts with oxygen to give trichloromethyl peroxy radical. Cytochrome P 450 2E1 is the enzyme responsible for this conversion. This radical binds covalently to the macromolecules and causes peroxidative degradation of lipid membrane of the hepatocytes. In this view, the reduction in the levels of SGOT and SGPT by the standard drug silymarin as well as with the tested compounds **5a** and **7a** is an indication of stabilization of plasma membrane as well as repairing of hepatic tissue damage caused by CCl_4. This effect is in agreement with commonly accepted view that serum levels of transaminases return to normal with the healing of hepatic parenchyma and regeneration of hepatocytes [19]. Alkaline phosphatase is the prototype of these enzymes that reflects the pathological alteration in biliary flow [20]. CCl_4-induced elevation of this enzymatic activity in the serum is in line with high level of serum bilirubin content. Silymarin and both tested compounds induced suppression of the increased serum ALP activity with the concurrent depletion of raised bilirubin suggests the possibility of the compounds **5a** and **7a** to have ability to stabilize biliary dysfunction in rat liver during hepatic injury with CCl_4. Thus, administration of silymarin and both compounds revealed its hepatoprotective activity against the toxic effect of CCl_4, which was also supported by histological studies.

The measurement of LPO is a convenient method to monitor oxidative cell damage. Because the lipid peroxidation is accelerated when free radicals are formed and scavenging of free radicals is one of the major antioxidation mechanisms to inhibit the chain reaction of LPO. This indicated the antilipid peroxidation and adaptive nature of the systems as brought about by silymarin as well as both compounds against the damaging effects of free radicals produced by CCl_4. During hepatic injury, superoxide radicals are generated at the site of damage and modulate SOD and CAT, resulting in the loss of activity and accumulation of superoxide radicals, which damage the liver. Decreased CAT activity is linked to exhaustion of the enzyme as a result of oxidative stress caused by CCl_4.

Reduction in liver GSH in CCl_4-treated rats as observed in this study indicates the damage to the hepatic cells. Administration of silymarin and chosen compounds **5a** and **7a** promoted the conversion of GSSG (oxidized glutathione) into GSH by

the reactivation of hepatic glutathione reductase enzyme, and SOD and CAT activities were brought to near normal levels in CCl_4-treated rats. The availability of sufficient amount of GSH thus increased the detoxification of reactive metabolites of CCl_4 through the involvement of glutathione peroxidase [21]. Therefore, the restoration of SOD, CAT, and GSH levels after the enduration of both compounds to such CCl_4-treated rats account for the antioxidant efficacy against free radicals. It might be attributed to the peculiar oxidizing power of both compounds, which can be explained on the basis of their strained structures [22]. The two benzene rings in phenanthrenequinone moiety are coaxial and owing to the normal spatial requirements of the carbonyl group; the diphenyl skeleton suffers a distortion or twisting which produces a strain within the molecule.

CCl_4-treated rats may potentiate focal hepatocyte damage and degeneration (Fig. 8). It is provoked by the increased production of a high reactive intermediate of CCl_4 like trichloromethyl free radical ($CCl_3^{\bullet}$), which is normally detoxified by endogenous glutathione, SOD, and CAT but in excess it may deplete these antioxidants, allowing the reactive intermediate to react with and destroy the hepatic cells and other cells [23].

These changes were very much reduced histopathologically in rats treated with CCl_4 and silymarin (Fig. 9) as well as with CCl_4 and compound **5a** (Fig. 10) and compound **7a** (Fig. 11) treated rats. As the alterations produced in the antioxidants level indicate involvement of deleterious oxidative changes, increased levels of these antioxidants would therefore be important in protection against toxicity.

CONCLUSION

It may be concluded that biochemical alterations observed in hepatic damage seems to be mainly due to an oxy-radical-mediated mechanism, involving lipid peroxidation, under conditions of reduced antioxidant levels that scavenge superoxide, hydrogen peroxide, and lipid peroxides. The results yet available are encouraging vis-à-vis standard drug silymarin and suggest that compounds **5a** and compound **7a** may be helpful in quenching free radicals by oxidizing them and induction of an in vivo antioxidant defense system.

EXPERIMENTAL

The uncorrected melting points were taken in open glass capillaries. The IR spectra were recorded on a Nicolet Magna IR spectrometer model 550 in KBr pellets, and band positions are reported in wave numbers (cm^{-1}). The ^1H NMR spectra and ^{13}C NMR spectra have been recorded on a Bruker DRX-300 MHz and 75.47 MHz models, respectively in $CDCl_3$ and (DMSO, 300 MHz) using tetramethylsilane as an internal standard. The chemical shifts (δ) are given in ppm. The mass spectra were recorded on a JEOL-SX 102 (FAB). Most of the spectra were recorded at Central Drug Research Institute, Lucknow, India. Elemental analyses were performed on a Perkin Elmer series C, H, N, S analyzer 2400. The solvents were purified by standard procedures [24, 25]. The optical rotations $^{20}[\alpha]_D$ were measured on a D line of Na lamp at 5893 Å wavelength, at 20°C in 1 g concentration using chloroform as solvent. Acetonitrile was dried by heating at reflux temperature with anhydrous calcium chloride for 5–6 h and then distilled it. Phenanthrenequinone, TCA, L-proline, and pipecolinic acid were purchased from Merck and Aldrich and used as supplied. Column chromatography was performed on silica gel 60 (Merck).

Computational Details

All calculations were carried out at MOPAC 6 program using AM1 Hamiltonians on PCL-Pentium 4, PC model for Windows, version 5.13 Serena software was used as a graphical interface for drawing and visualizing all structures and for preparing input files for MOPAC 6. The energy terms are given in kcal/mol.

Synthesis of Compounds **4a–8c**

*A Representative Method for the Synthesis of Cycloadduct (5S, 8R)-Spiro-{7-phenyl-1-aza-3-thia-bicyclo[3,3,0]-6-octene-8,1′-phenanthrene-2′-one (**4a**).* A mixture of phenanthrenequinone **1** (0.416 g; 2.0 mmol), thiazolidine-4-carboxylic acid (0.266 g; 2.0 mmol), and phenyl acetylene (0.219 g, 2.0 mmol) in equimolar amount was heated at reflux temperature under a nitrogen atmosphere for 22 h in dry acetonitrile. After completion of the reaction as monitored by TLC, unreacted acid was removed by filtration. The filtrate was evaporated in vacuo to half of its volume. The crude product so obtained was purified using column chromatography over silica gel, whereby chloroform/ethyl acetate (3:1) fraction afforded the cycloadduct **4a** as bright yellow crystalline solid in 70% yield; mp 200°C; ^1H NMR ((DMSO, 300 MHZ), 300 MHz) δ: 1.86 (d, 5-H, 1H), 2.25 (d, 4-H, 2H), 2.90 (br m 2-H + 6-H, 4H), 7.26–8.21 (m, 13H, 5 ArH + 3′-H to 10′-H). ^{13}C NMR (DMSO, 75.47 MHz) δ: 180.2 (>C=O), 136.0–128.3 (6 ArC + C-3′–C-10′), 128.2, 123.9 (C=C), 89.5 (C-8),

66.6 (C-5), 59.0 (C-2), 49.0 (C-4) ppm. IR (KBr) (ν_{max}) cm^{-1}: 3050, 1675, 1290, 650. Mass *m/z*: 381 [M^+] (35%), 353 [$M^+ - CO$] (43%), 279 [$M^+ - C_8H_6$] (100%), 152 [$M^+ - C_{13}H_{11}NOS$] (40%). $^{20}[\alpha]_D$ ($CHCl_3$) = 50. Elemental anal. (%) Calcd: C, 78.74; H, 4.98; N, 3.67; Found: C, 78.82; H, 4.72; N, 3.45.

*(5S,8R)-Spiro-{6,7-diphenyl-1-aza-3-thia-bicyclo-[3,3,0]-6-octene-8,1′-phenanthrene}-2′-one (**5a**).* A mixture of phenanthrenequinone (**1**) (0.41 g, 2.0 mmol), thiazolidine-4-carboxylic acid (**2a**) (0.26 g, 2.0 mmol), and diphenyl acetylene (0.35 g; 2.0 mmol) in the molar ratio 1:1:1 was heated at reflux temperature under nitrogen atmosphere for 22 h in dry acetonitrile (50 mL). The completion of the reaction was judged by TLC. The unreacted acid was filtered off, and the filtrate was evaporated in vacuo to half of its volume. After failing in several attempts to crystallize the product from various solvent mixtures, the product was purified using column chromatography over silica gel whereby cycloadduct **5a** was obtained as pale yellow crystals in 75% yield; mp 156°C; ^{1}H NMR ((DMSO, 300 MHz) δ: 1.86 (d, 4-H, 2H), 2.89 (s, 2-H, 2H), 4.97 (t, 5-H, 1H), 7.20–8.21 (m, 18ArH) ppm. IR (KBr), ν_{max} (cm^{-1}): 3065, 1675, 1285, 930, 680. $^{20}[\alpha]_D$ ($CHCl_3$) = 47. Elemental anal. (%) Calcd: C, 81.40; H, 5.03; N, 3.06; Found: C, 80.92; H, 4.89; N, 2.83.

*(5S,8R)-Spiro-{6-methyl-7-phenyl-1-aza-3-thia-bicyclo-[3,3,0]-6-octene-8,1′-phenanthrene}-2′-one (**6a**).* The cycloadduct was obtained in 76% yield as brown solid; mp 144°C; ^{1}H NMR (DMSO, 300 MHz) δ: 1.76 (d, 4-H, 2H), 2.25 (s, CH_3, 3H), 2.89 (br m, 2-H, 2H), 3.86 (d, 5-H, 1H), 7.29 (t, 5′H + 8′H), 7.50 (m, 5 ArH), 7.70 (t, 4′H + 9′H), 8.01 (d, 3′H + 10′H), 8.18 (d, 6′H + 7′H) ppm. ^{13}C NMR (DMSO, 75.47 MHz) δ: 180.1 (>C=O), 135.9–129.4 (6 ArC + C-3′–C-10′), 128.5, 123.8 (C=C), 84.1 (C-8), 62.1 (C-5), 52.0 (C-2), 39.8 (C-4), 14.0 (CH_3). IR (KBr) ν_{max} (cm^{-1}): 3055, 1675, 1280, 920, 660. $^{20}[\alpha]_D$ ($CHCl_3$) = 42. Elemental anal. (%) Calcd.: C, 78.98; H, 5.31; N, 3.54; Found: C, 78.13; H, 5.12; N, 3.24.

*(5S,8R)-Spiro-{6-ethoxycarbonyl-7-phenyl-1-aza-3-thia-bicyclo-[3,3,0]-6-octene-8,1′-phenanthrene}-2′-one (**7a**).* The compound was obtained as black solid in 70% yield; mp 154°C; ^{1}H NMR (DMSO, 300 MHz) δ: 1.36 (t, CH_3, 3H), 2.00 (d, 4-H, 2H), 2.92 (br s, 2-H, 2H), 3.94 (d, J = 6.89 Hz, 5-H, 1H), 4.30 (q, J = 7.16 Hz, OCH_2, 2H), 7.26–8.18 (m, 13ArH). IR (KBr) ν_{max} (cm^{-1}): 3060, 1680, 1670, 1280, 930, 660. $^{20}[\alpha]_D$ ($CHCl_3$) = 40. Elemental Anal. (%) Calcd: C, 74.17; H, 5.07 N, 3.09; Found: C, 75.22; H, 4.97; N, 2.99.

*(5S, 7S, 8R)-Spiro-{7-methoxycarbonyl-1-aza-3-thia-bicyclo-[3,3,0]-octane-8,1′-phenanthrene}-2′ one (**8a**).* The cycloadduct was obtained in 73% yield as dark brown crystals; mp 182°C; ^{1}H NMR (DMSO, 300 MHz) δ: 0.85 ((d, 6-H, 2H), 1.25 (t, 4-H, 2H), 1.84 (t, 7-H, 1H), 2.10 (dd, 2-H, 2H), 2.62 (s, OCH_3, 3H), 4.12 (m, 5-H, 1H), 7.39 (t, J = 7.23 Hz, 5′-H + 8′-H, 2H), 7.72 (t, J = 8.13 Hz, 4′H + 9′ H, 2H), 8.01 (d, J = 8.23 Hz, 3′-H + 10′-H, 2H), 8.19 (d, J = 7.69 Hz, 6′-H + 7′-H, 2H) ppm.

IR (KBr) ν_{max} (cm^{-1}): 3075, 1690, 1650, 1275, 1230, 930, 675. $^{20}[\alpha]_D$ ($CHCl_3$) = 51. Elemental anal. (%) Calcd.: C, 69.04; H, 5.20; N, 3.83; Found: C, 68.42; H, 4.99; N, 3.74.

*(2R, 5S)-Spiro-{3-phenyl-1-aza-bicyclo-[3,3,0]-3-octene-2,1′-phenanthrene}-2′-dione (**4b**).* The compound was obtained in 75% yield as shining brown crystals; mp 120°C; ^{1}H NMR (DMSO, 300 MHz) δ: 1.25 (m, 6-H, 2H), 2.08 (m, 7-H, 2H), 2.72 (t, 8-H, 2H), 3.07 (q, 5-H, 1H), 3.49 (d, 4-H, 1H), 7.25–8.36 (m, 13 H, 5 ArH+ 3′-H to 10′-H) ppm. IR (KBr) ν_{max} (cm^{-1}): 3030, 2920, 1700, 1300, 790. $^{20}[\alpha]_D$ ($CHCl_3$) = 54. Elemental anal. (%) Calcd.: C, 85.95; H, 5.78; N, 3.85; Found: C, 85.29; H, 5.62; N, 3.79.

*(2R, 5S)-Spiro-{3,4-diphenyl-1-aza-bicyclo-[3, 3, 0]-3-octene-2,1′-phenanthrene}-2′-one (**5b**).* The cycloadduct was obtained as black crystals in 76% yield; mp 178°C; ^{1}H NMR (DMSO, 300 MHz) δ: 1.64 (m, 7-H, 2H), 1.89 (t, 6-H, 2H), 2.05 (t, 5-H, 1H), 4.67 (t, 8-H, 2H), 7.33–8.09 (m, 18ArH) ppm. IR (KBr) ν_{max} (cm^{-1}): 3020, 2910, 1680, 1400, 800. $^{20}[\alpha]_D$ ($CHCl_3$) = 62. Elemental anal. (%) Calcd.: C, 87.47; H, 5.69; N, 3.18; Found: C, 87.13; H, 5.56; N, 2.91.

*(2R, 5S)-Spiro-{4-methyl-3-phenyl-1-aza-bicyclo-[3,3,0]-3-octene-2,1′-phenanthrene}-2′-one (**6b**).* The cycloadduct was obtained in 77% yield as coffee brown solid; mp 192°C; ^{1}H NMR (DMSO, 300 MHz) δ: 0.88 (m, 7-H, 2H), 1.29 (m, 6-H, 2H), 2.05 (s, CH_3, 3H), 2.20 (t, 8-H, 2H), 3.48 (t, 5-H, 1H), 7.14–8.08 (m, 13ArH). IR (KBr) ν_{max} (cm^{-1}): 3010, 1690, 1275, 820. $^{20}[\alpha]_D$ ($CHCl_3$) = 59. Elemental anal. (%) Calcd: C, 85.94; H, 6.10; N, 3.71; Found: C, 84.79; H, 5.87; N, 3.59.

*(2R,5S)-Spiro-{4-ethoxycarbonyl-3-phenyl-1-aza-bicyclo-[3,3,0]-3-octene-2,1′-phenanthrene}-2′-one (**7b**).* The cycloadduct was obtained as brown powder in 74% yield; mp 188°C; ^{1}H NMR (DMSO, 300 MHz) δ: 1.24 (q, CH_3, 3H), 1.43 (m, 6-H + 7-H, 4H), 1.69 (t, 8-H, 2H), 3.71 (q, J = 6.96 Hz, OCH_2, 2H), 4.30 (t, J = 7.14 Hz, 5-H, 1H), 7.39 (m, 5 ArH), 7.47 (t, 5′H + 8′H, 2H), 7.73 (t, 4′H + 9′H, 2H),

8.02 (d, 3′H + 10′H, 2H), 8.19 (d, 6′H + 7′H, 2H). ^{13}C NMR (DMSO, 75.47 MHz) δ: 190.1 (>C=O), 180.2 (O–C=O), 135.9–123.1 (6 ArC + C-3′–C-10′), 122.2, 121.5 (C=C), 86.5 (C-2), 66.0 (OCH_2), 62.0 (C-5), 49.8 (C-8), 41.8 (C-6), 35.7 (C-7), 19.1 (CH_3). IR (KBr) ν_{max} (cm^{-1}): 3075, 2950, 1700, 1680, 1270, 1190, 800. Mass *m/z*: 435 [M^+] (50%), 261 [$M^+ - C_{11}H_{10}O_2$] (100%), 233 [$M^+ - C_{12}H_{10}O_3$] (55%), 180 [$M^+ - C_{16}H_{17}NO_2$] (65%), 152 [$M^+ - C_{17}H_{17}NO_3$] (45%). $^{20}[\alpha]_D$ ($CHCl_3$) = 60. Elemental anal. (%) Calcd: C, 80.01; H, 5.74; N, 3.21 Found: C, 79.75; H, 5.54; N, 3.18.

(2R, 3R, 5S)-Spiro-{3-methoxycarbonyl-1-aza-bicyclo-[3,3,0]-octane-2,1′-phenanthrene} -2′-one (**8b**). The compound was obtained as dark brown solid in 74% yield; mp 130°C; ^{1}H NMR (DMSO, 300 MHz) δ: 1.52 (s, 7-H + 3-H, 4H), 1.85 (m, 6-H, 2H), 2.02 (m, 5-H + 4-H, 3H), 2.64 (s, 8-H, 2H), 2.77 (s, OCH_3, 3H), 7.35 (t, J = 7.04 Hz, 5′H + 8′H, 2H), 7.59 (t, J = 8.26 Hz, 4′H + 9′H, 2H), 7.98 (d, J = 8.42 Hz, 3′H + 10′H, 2H), 8.08 (d, J = 7.55 Hz, 6′H + 7′H, 2H). IR (KBr) ν_{max} (cm^{-1}): 3040, 2950, 1720, 1700, 1375, 1230. $^{20}[\alpha]_D$ ($CHCl_3$) = 48. Elemental anal. (%) Calcd: C, 76.08; H, 6.05; N, 4.03; Found: C, 75.94; H, 5.93; N, 3.91.

(6S, 9R)-Spiro-{8-phenyl-1-aza-bicyclo-[4,3,0]-7-nonen-9,1′-phenanthrene}-2′-one (**4c**). The compound was obtained as brown powder in 74% yield; mp 182°C; ^{1}H NMR (DMSO, 300 MHz) δ: 0.79 (m, 3-H, 2H), 1.80 (s, 4-H, 2H), 2.10 (q, 5-H, 2H), 2.77 (t, 2-H, 2H), 3.71 (q, 6-H, 1H), 4.30 (t, 7H, 1H), 7.26–8.21 (m, 13 H, 5 ArH + 3′-H to 10′-H). ^{13}C NMR (DMSO, 75.47 MHz) δ: 180.7 (>C=O), 143.8–130.1 (6 ArC + C-3′–C-10′), 128.8, 124.4 (C=C), 85.9 (C-9), 80.6 (C-6), 66.3 (C-2), 47.4 (C-5), 35.8 (C-4), 28.4 (C-3) ppm. IR (KBr) ν_{max} (cm^{-1}): 3060, 2910, 1675, 1235, 775. $^{20}[\alpha]_D$ ($CHCl_3$) = 63. Elemental anal. (%) Calcd: C, 85.94; H, 6.10; N, 3.71; Found: C, 85.41; H, 5.88; N, 3.55.

(6S,9R)-Spiro-{7,8-diphenyl-1-aza-bicyclo-[4,3,0]-7-nonen-9,1′-phenanthrene}-2′-one (**5c**). The compound was obtained as chocolate brown solid in 72% yield; mp 170°C; ^{1}H NMR (DMSO, 300 MHz) δ: 1.25 (q, 5-H, 2H), 1.35 (m, 4-H, 2H), 2.01 (m, 3-H, 2H), 3.34 (t, 2-H, 2H), 4.31 (t, 6-H, 1H), 7.21–8.62 (m, 18ArH) ppm.

IR (KBr) ν_{max} (cm^{-1}): 3060, 2860, 1670, 1235. $^{20}[\alpha]_D$ ($CHCl_3$) = 54. Elemental anal. (%) Calcd: C, 87.41; H, 5.96; N, 3.09; Found: C, 86.92; H, 5.89; N, 2.93.

(6S,9R)-Spiro-{7-methyl-8-phenyl-1-aza-bicyclo-[4,3,0]-7-nonen-9,1′-phenanthrene}-2′-one (**6c**). The compound was obtained as camel yellow crystals in 67% yield; mp 200°C; ^{1}H NMR (DMSO, 300 MHz) δ: 1.25 (s, 2-H, 2H), 1.35 (m, 3-H + 4-H, 4H), 1.64 (br m, 5-H, 2H), 2.01 (s, CH_3, 3H), 4.29 (t, 6-H, 1H), 7.38 (m, 2 × *m*-ArH + 1 × *p*-ArH, 3H), δ: 7.49 (t, 5′H + 8′H, 2H), 7.58 (d, 2 × *o*-ArH, 2H), 7.71 (t, 4′H + 9′H, 2H), 8.03 (d, 3′H + 10′H, 2H), 8.21 (d, 6′H + 7′H, 2H) ppm IR (KBr) ν_{max} (cm^{-1}): 3050, 1655, 1240, 770. $^{20}[\alpha]_D$ ($CHCl_3$) = 48. Elemental Anal. (%) Calcd: C, 85.93; H, 6.39; N, 3.58; Found: C, 85.23; H, 6.19; N, 3.42.

(6S, 9R)-Spiro-{7-ethoxycarbonyl-8-phenyl-1-aza-bicyclo-[4,3,0]-7-nonen-9,1′-phenanthrene}-2′-one (**7c**). The compound was obtained as dark brown solid in 71% yield; mp 154°C; ^{1}H NMR (DMSO, 300 MHz) δ: 1.24 (t, CH_3, 3H), 1.36 (t, 3-H, 2H), 1.67 (br m, 4-H + 5-H, 4H), 2.02 (d, 2-H, 2H), 3.71 (q, J = 6.96 Hz, OCH_2, 2H), 4.29 (t, J = 7.24 Hz, 6-H, 1H), 7.36 (m, 2 × *m* ArH + 1 × *p*-ArH, 3H), δ: 7.47 (t, 5′H + 8′H, 2H), 7.58 (d, 2 × *o*-ArH, 2H), 7.75 (t, 4′H + 9′H, 2H), 8.02 (d, 3′H + 10′H, 2H), 8.19 (d, 6′H + 7′H, 2H) ppm. ^{13}C NMR (DMSO, 75.47 MHz) δ: 180.1 (>C=O), 174.0 (O–C=O), 135.9–128.4 (6 ArC + C-3′–C-10′), 123.8, 119.5 (C=C), 85.9 (C-9), 80.6 (C-6), 70.1 (OCH_2), 62.0 (C-2), 54.0 (C-5), 35.7 (C-4), 25.4 (C-3), 14.0 (CH_3). IR(KBr) ν_{max}(cm^{-1}): 3055, 2855, 1690, 1670, 1290, 1235, 760. Mass *m/z*: 449 [M^+] (38%), 275 [$M^+ - C_{11}H_{10}O_2$] (100%), 192 [$M^+ - C_{16}H_{19}NO_2$] (52%), 180 [$M^+ - C_{17}H_{19}NO_2$] (47%), 152 [$M^+ - C_{18}H_{19}NO_3$] (34%). $^{20}[\alpha]_D$ ($CHCl_3$) = 68. Elemental anal. (%) Calcd: C, 80.17; H, 6.01; N, 3.11; Found: C, 79.92; H, 5.91; N, 2.98.

(6S,8S,9R)-Spiro-{8-methoxycarbonyl-1-aza-bicyclo-[4,3,0]-nonan-9,1′-phenanthrene}-2′-one (**8c**). The compound was obtained as orange needles in 72% yield; mp 166°C; ^{1}H NMR (DMSO, 300 MHz) δ: 2.30 (d, 5-H, 2H), 2.32 (m, 3-H + 4-H, 4H), 2.38 (t, 2-H, 2H), 2.98 (br m, 7-H + 8-H, 3H), 3.49 (m, 6-H, 1H), 4.64 (s, OCH_3, 3H), 7.47 (t, J = 7.34 Hz, 5′H + 8′H, 2H), 7.73 (t, J = 8.27 Hz, 4′H + 9′H, 2H), 8.02 (d, J = 8.23 Hz, 3′H + 10′H, 2H), 8.19 (d, J = 7.71 Hz, 6′H + 7′H, 2H) ppm IR (KBr) ν_{max} (cm^{-1}): 3060, 1680, 1650, 1290, 1220, 760. $^{20}[\alpha]_D$ ($CHCl_3$) = 62. Elemental anal. (%) Calcd: C, 76.45; H, 6.37; N, 3.87; Found C, 76.12; H, 5.96; N, 3.79.

The cycloadducts **4a–8c** are optically active, and their specific rotations $^{20}[\alpha]_D$ were in the range 40°–68° using chloroform ($CHCl_3$) as solvent.

Antioxidant Activity Procedure

Methodology.

Animals. Adult male, Wistar strain, albino rats weighing 150–170 g were used. The animals were housed in standard laboratory conditions and were maintained on rat diet (Lipton India Ltd.) and tap water ad libitum under a natural light–dark (12L:12D) cycle. The study was approved by the departmental ethical committee.

Selection of Dose Level of Compounds **5a** *and* **7a**. The compounds **5a** and **7a** were found to be a practically nontoxic when administered orally to rats, and LD_{50} value of both compounds was found to be higher than 40 mg/kg body weight. The double of minimum dose level of both compounds, namely 10 mg/kg body weight, was used for experimentation.

Experimental Design. After 15 days of acclimatization, the animals were divided into following groups with six rats in each group.

Group I: Vehicle-treated rats were kept on normal diet and served as control.

Group II: Rats were intoxicated with CCl_4 (1.0 mL/kg body weight/once a week with olive oil, intraperitoneally, 1:1) for 15 days.

Group III: Rats received 10 mg/kg body weight/day, orally with olive oil of silymarin and CCl_4 for 15 days.

Group IV: Rats received 10 mg/kg body weight/day, orally with olive oil of compound **5a** and CCl_4 for 15 days.

Group V: Rats received 10 mg/kg body weight/day, orally with olive oil of compound **7a** and CCl_4 for 15 days.

Biochemical Analysis. After the 24 h of last dose delivery, all rats of each treated group were autopsied and blood was collected by cardiac puncture. Serum was separated by centrifugation at 2500 rpm for 20 min at 37°C and was analyzed for SGOT, SGPT (aminotransferases), ALP, and total bilirubin using diagnostic kits. All kits were purchased from Span Diagnosis Ltd. (Surat, India). The standard drug silymarin (known antioxidant) was purchased from German Remedies Ltd. (Mumbai, India).

After collection of blood, liver was immediately excised, washed with cold saline, blotted and a part of it was minced and homogenized for SOD [26], CAT [27], GSH [28], and LPO [29] determination, respectively.

The remaining part of liver was fixed in 10% formalin solution, dehydrated with different ethanol solutions (50%–100%), embedded in paraffin wax then cut into 5 μm sections and stained with hematoxylin–eosin dye for photomicroscopic observations.

Statistical Analysis. All results were expressed as mean ± SEM and were analyzed using the student's *t*-test. A probability value of $p \leq 0.05$ was considered as significant.

REFERENCES

[1] Huisgen, R. Angew Chem 1963, 75(13), 604.
[2] (a) Pandey, G.; Banerjee, P.; Gadre, S. R. Chem Rev 2006, 106(11), 4484; (b) Gothelf, Kurt V. In Cycloaddition Reactions in Organic Synthesis; Kobayashi, S.; Jorgensen, K. A.; (Eds.); Wiley-VCH; Weinheim, Germany, 2002; Ch. 6, p. 211; (c) Gothelf, K. V.; Jorgensen, K. A. Chem Rev 1998, 98(2), 863; (d) Gribble, G. W. In Comprehensive Heterocyclic Chemistry; Katritzky, A. R.; Rees, C. W.; Scriver, E. F. V.; (Eds.); Pergamon; Oxford, UK, 1996; Vol. 2, p. 207.
[3] (a) Harwood, L. M.; Vickers, R. J. In Synthetic Applications of 1,3-Dipolar Cycloaddition Chemistry Toward Heterocycles and Natural Products; Padwa, A.; Pearson, W. H. (Eds.); Wiley: New York, 2003; Ch. 3, p. 169; (b) Najera, C.; Sansano, J. M. Curr Org Chem 2003, 7(11), 1105; (c) Tsuge, O.; Kanesmasa, S. In Advances in Cycloaddition; Curran, D. P.; (Ed.); JAI Press; Greenwich, CT, 1993; Vol. 3, p. 99; (d) Pearson, W. H.; Stoy, P. SynLett 2003, 903.
[4] (a) Londhe, A. V.; Gupta, B.; Kohli, S.; Pardasani, P.; Pardasani, R. T. Z Naturoforsch B 2006, 61b, 213; (b) Pardasani, R. T.; Pardasani, P.; Jain, A.; Arora, K. Indian J Chem B 2005, 44, 1204; (c) Pardasani, R. T.; Pardasani, P.; Chaturvedi, V.; Yadav, S. K.; Saxena, A.; Sharma, I. Heteroatom Chem 2003, 14, 36; (d) Pardasani, R. T.; Pardasani, P.; Yadav, S. K.; Bharatam, P. V. J Heterocycl Chem 2003, 40, 557; (e) Pardasani, R. T.; Pardasani, P.; Sherry, D.; Chaturvedi, V. K. Synth Commun 2002, 40, 435.
[5] (a) Zhu, Y. Z.; Huang, S. H.; Tan, K. H.; Sun, J.; Whiteman, M.; Zhu, Y. C. Nat Prod Rep 2004, 21, 478; (b) Ip, Sui Po; Yang, H.; Sun, H.-D.; Che, C.-T. Planta Med 2002, 68, 1077; (c) Cao, E. H.; Liu, X. Q.; Wang, J. J.; Xu, N. F. Free radical Biol Med 1996, 20 (6), 801; (d) Jiang, W.; Zhao, Y.; Zhao, B.; Wan, Q.; Xin, W. Acta Biophys Sinica 1994, 10, 685; (e) Wu, T.-W.; Zeng, L.-H.; Fung, K.-P.; Wu, J.; Pang, H.; Grey, A. A.; Weisel, R. D.; Wang, J. Y. Biochem Pharmacol 1993, 46 (12), 2327.
[6] (a) Pranham, M. J. Biochem Pharmacol 1999, 58, 209; (b) Kamal, A. J Org Chem 1991, 56, 2237; (c) Dressman, B. A.; Fritz, J. E.; Hammond, M.; Hornback, W. J.; Kaldor, S. W.; Kalish, V. J.; Munroe, J. E.; Reich, S. H.; Tatlock, J. H. PCT Int. Appl. WO 95, 1995, 09, 843, US Appl 133, 543 Chem Abstr 1998, 123, 256539v; (d) Vicchietti, V.; Colle, R.; Dondio, G.; Giordani, A. Eur Pat Appl 1991, EP 447, 704.

[7] Navarro, A.; Sanchez Pino, M.-J.; Gomez, C.; Bandez, M. J.; Cadenas, E.; Boveris, A. Antioxid Redox Signal 2007, 9, 131.
[8] De la Funte, M.; Ferrandez, D.; Munoz, F.; de Juan, E.; Miquel, J. Mech Ageing Dev 1993, 68(1–3), 27.
[9] (a) De la Funte, M.; Miquel, J.; Catalan, M. P.; Victor, V. M.; Guayerbas, N.; Free Radical Research 2002, 36, 119; (b) De la Fuente, M.; Ferrandez, M D.; Del Rio, M.; Sol Burgos, M.; Miquel, J. Mech Ageing Dev 1998, 104, 213.
[10] Del Rio, M.; Ruedas, G.; Medina, S.; Victor, V. M.; De la Fuente, M. Life Sci, 1998, 63, 871.
[11] Correa, R.; Blanco, B.; Del Rio, M.; Victor, V.; Guayerbas, N.; Medina, S.; De La Fuente, M. Bio Factors, 1999, 10, 195.
[12] Amornaksa, K.; Grigg, R.; Gunaratne, H. Q. N.; Kemp, J.; Sridharan, V.; J Chem Soc, Perkin Trans I 1987, 2285.
[13] Coulter, T.; Grigg, R; Malone, J. F.; Sridharan, V. Tetrahedron Lett 1991, 32, 5417.
[14] Ardill, H.; Dorrity, M. J. R.; Grigg, R.; Leon-Ling, M. S.; Malone, J. F.; Sridharan, V.; Thianpatanagul, S. Tetrahedron Lett 1990, 46(18), 6433.
[15] Yeler, H.; Tahtabas, F.; Candan, F. Cell Biochem Funct 2005, 23(2), 137.
[16] Weber, L. W. D.; Boll, M.; Stampfl, A. Crit Rev Toxicol 2003, 33, 105.
[17] Youdim, K. A.; Joseph, J. A. Free Radical Biol Med 2001, 30, 583.
[18] Recknagel, R. O. Life Sci 1983, 33 (5), 401.
[19] Thabrew, M. I.; Joice, P. D. T. M.; Rajatissa, W.; Planta Med 1987, 53, 239.
[20] Ploa, G. L.; Hewitt, W. R.; Wallace, H. A. (Ed.) Principle and Methods of Toxicology, Vol II; Raven Press: New York, 1989; p. 399.
[21] Kamalakkannan, N.; Rukkumani, R.; Varma, P. S.; Viswanathan, P.; Rajasekharan, K. N.; Menon, V. P. Basic Clin Pharmacol Toxicol 2005, 97(1), 15.
[22] Fieser, L. F. J Org Chem 1929, 3101.
[23] Pessayre, D.; Larrey, D.; Brentano, F. C.; Benhamon, J. P. J Antimicrob Chemother 1985, 16, 181.
[24] Perrin, D. D.; Armarego, W. L. F.; Perrin, D. R. Purification of Laboratory Chemicals, 2nd ed.; Pergamon Press: Oxford, 1998.
[25] Vogel, A. I. Vogel's Text Book of Practical Organic Chemistry, 4th ed.; ELBS Longman: London, 1984.
[26] Marklund, S.; Marklund, G. Eur J Biochem 1974, 47, 469.
[27] Aebi, H.; Colowick, S. P.; Kaplan, N. O. Eds. In Methods in Enzymology. Academic Press: New York, 1984; Vol. 105, p. 121.
[28] Moron, M. S.; De Pierre, J. W.; Mannervick, B. Biochim Biophys Acta 1979, 582, 6778.
[29] Ohkawa, H.; Ohishi, N.; Yagi, K. Anal Biochem 1979, 95(2), 351.